ELSEVIER

Ceramics International 30 (2004) 435–439

CERAMICS INTERNATIONAL

www.elsevier.com/locate/ceramint

# The fabrication of reaction-formed silicon carbide with controlled microstructure by infiltrating a pure carbon preform with molten Si

YanXiang Wang*, ShouHong Tan, DongLiang Jiang

*State Key Laboratory of High Performance Ceramics and Superfine Microstructures, Shanghai Institute of Ceramics, Chinese Academy of Sciences, Shanghai 200050, PR China*

Received 6 April 2003; received in revised form 12 April 2003; accepted 20 May 2003

**Abstract**

This paper describes the production of shaped silicon carbide based ceramic materials by in situ reaction of silicon with fine, ultra-uniform porous carbon skeletons that were produced from liquid polymer solutions without any particulate additions. Three typical types of carbon preforms (spherical carbon particulates, crosslinked network carbon, and lamellate carbon particulates) were infiltrated with molten Si. The morphologies and mechanical properties of corresponding reaction-formed silicon carbide (RFSC) ceramics have been investigated. The results revealed that the RFSC obtained by molten Si reaction with the porous carbon preform with discrete and spherical carbon particulates has the most uniform microstructure, the highest flexural strength ($410 \pm 30$ MPa) and the lowest amount of residual Si (approximately 12 wt.%). The general feature of a fracture surface showed the typically brittle failure in those materials.


*Keywords:* B. Electron microscopy; C. Mechanical properties; Reaction-formed silicon carbide

## 1. Introduction

The reaction-bonded silicon carbide (RBSC) process involves infiltration of liquid silicon or Si alloy into porous carbon preform with simultaneous chemical reaction. The SiC product is attractive for its high thermal conductivity, thermal resistance, strength, fracture toughness, and wear resistance. Furthermore, the processing time is short and the SiC can be produced with dense and near-net shape without external pressure at relatively low temperature, compared with the other sintering method. It is an obvious candidate for ceramic components in gas turbine engines, heat exchangers, and wear resistant seals. Commercially available reaction-bonded silicon carbide is fabricated by the melt infiltration of silicon into preforms containing silicon carbide and carbon, which has been extensively studied in the past [1–7].

The process chosen in this paper is a variant of reaction-bonding, which has the potential advantages of yielding high accuracy shaped objects. The major difference between this approach and reaction-bonded is that no particulate material is processed in making the shaped body. Instead, the body is made from low viscosity castable liquid polymer which is converted to a pure carbon skeleton with controlled porosity after pyrolysis. Subsequently, the skeleton is reacted with silicon to form the silicon carbide. The control of pore size distribution and maximum carbon dimension within the skeleton is excellent and allow a greater degree of control of the subsequent siliconization. The manipulation of the skeleton parameters is through variation of chemical variables such as concentrations, times and temperatures and not mechanical processes such as grinding, mixing and pressing. One major attribute of this technique is the avoidance of porosity defects and residual Si. Residual silicon of relatively low melting point is detrimental to high-temperature application of the product.

This method was invented by Hucke [8,9], discussed in Refs. [10–12]. However, there are no systemic studies about the effects of carbon preform on the properties of reaction-formed silicon carbide (RFSC). In this paper, the effects of carbon preform microstructure on the

* Corresponding author. Tel.: +86-21-5241-1044; fax: +86-21-5241-3903.

*E-mail address:* yxwang@mail.sic.ac.cn (YanXiang Wang).

0272-8842/$30.00 
doi:10.1016/S0272-8842(03)00128-7

morphologies and mechanical properties of the reaction-formed silicon carbides (RFSC) are reported.

## 2. Experimental

### 2.1. Samples preparation

The porous carbon preforms were synthesized from a mixture of furfuryl resin, furfuryl alcohol, diethyleneglycol and triethyleneglycol, water and paratoluene sulfonic acid (PTSA).This mixture is polymerized to form a porous solid polymer, which is heated up to 700 °C to yield a porous carbon preform. By varying the ratios of the constituents in the polymer system or changing the polymerizing conditions, porous carbon performs with a wide variation in pore volumes, pore sizes, and morphologies have been obtained. Machined porous carbon performs were reaction infiltrated with Si at 1550 °C for 30 min in a vacuum furnace.

### 2.2. Analysis

The morphologies of samples were characterized by optical and scanning electron microscopy. Pore size distribution, bulk density and apparent porosity of porous carbon preforms were examined by mercury porosimetry (PoreSizer 9320, Micromeritics, USA). The surface areas of the porous carbon preforms were characterized by nitrogen adsorption-desorption isotherms obtained with an automatic adsorption instrument (ASAP 2010, Micromeritics, USA) at 77 K.

Powder X-ray diffraction analysis was used for identification of the different phases. The amount of residual silicon was calculated by weighing the samples before and after etching (17 h in a 70 wt.%HF/30 wt.%$HNO_3$ solution at room temperature). Three-point flexural testing of reaction-formed silicon carbide materials was performed with an Instron 1195 machine. The flexure specimens were 36×4×3 mm in length, width and height respectively. A loading rate of 0.5 mm·min$^{-1}$ was employed in the flexural test.

## 3. Results and discussion

### 3.1. Characterization of carbon performs

SEM micrographs of the three types of porous carbon preforms examined in this study are given in Fig. 1. These micrographs show uniform struts and pores indicating the ability of this process to produce carbon preforms with homogeneous microstructures. These preforms have different pore and carbon particle sizes. Fig. 1(a) shows a preform with an average pore size of about 1.81 μm and a bulk density of 0.86 g cm$^{-3}$. This preform has been labeled as CA-1. The preform in Fig. 1(b) has an average pore size of about 1.12 μm and a bulk density of 0.86 g·cm$^{-3}$.The preform shown in Fig. 1(c) has an average pore size of 0.33 μm and a bulk density of 0.80 g·cm$^{-3}$. These two type preforms have been labeled as CA-2 and CA-3 respectively. The properties of the three performs are summarized in Table 1.

Mercury porosimetry results for the three carbon preforms are given in Figs. 2 and 3. A plot of the cumulative intrusion versus pore diameter is given in Fig. 2. The steep rises in the curves indicate very narrow pore size distributions. The sample CA-3 shows no measurable intrusion volume due to pores with diameters above 0.5 μm. A plot of the incremental intrusion versus the pore diameter is presented in Fig. 3. This plot also emphasizes that the pore size distributions in the preforms are very narrow. Actually, the major contribution to the total pore volume of the preforms is from pores between 1 and 2 μm diameter for the sample CA-1, 0.5 and 2 μm diameter for the sample CA-2, and 0.1–0.5 μm diameter for the sample CA-3.

### 3.2. Microstructure and phase composition

The porous carbon preforms CA-1, CA-2 and CA-3 were infiltrated with Si under identical conditions. The samples of silicon infiltrated carbon preforms are denoted as RFA-1, RFA-2 and RFA-3, respectively. The optical and SEM micrographs of RFA-1, RFA-2 and RFA-3 are shown in Fig. 4. It is obvious that the morphologies are significantly different. Fig. 4(a) (optical micrographs of RFA-1) shows the complete conversion of carbon to silicon carbide. This microstructure shows a very uniform distribution of the residual silicon phase (white) throughout silicon carbide matrix (gray). In this composite, no porosity or residual carbon is visible. The grain size of SiC is approximately 3 μm, close to the carbon size scale in the starting perform. The amount of residual silicon in this material is estimated to be approximately 12 wt.%. Optical micrograph of the sample RFA-2 [Fig. 4(b)] shows the residual carbon (dark), which was closed by newly formed SiC (gray). Optical and SEM examination of the sample RFA-3 revealed a markly non-uniform overall microstructure with several distinct types of localized features. Some regions have the fine distribution of SiC in free Si matrix [Fig. 4(c) and (e)]. The grain size of silicon carbide is about 1–2 μm [Fig. 4(e)]. Some regions take the form of silicon carbide grain coarsening and formation of silicon veins and lakes [the white areas in Fig. 4(d)]. The scale of coarse-grained silicon carbide is observed to be about 5–8μm [Fig. 4(f)].

The reaction of silicon with carbon is exothermic. The exothermic degree of this reaction depends on a number of parameters including the surface area of the reactant, pore size, pore volume of the porous carbon preforms

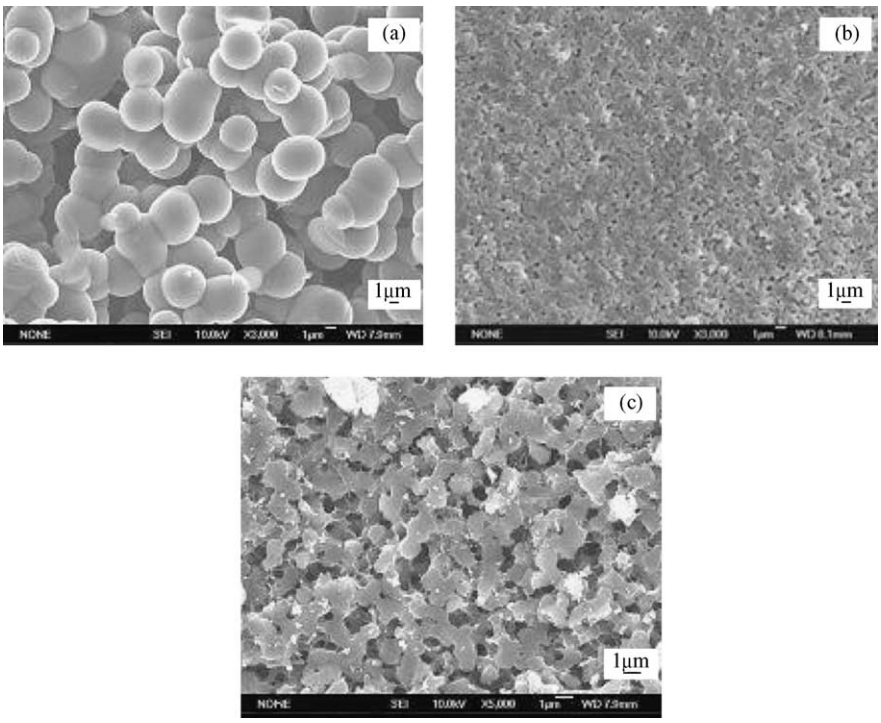


Fig. 1. SEM micrographs of porous carbon performs (a)CA-1 (b) CA-2 (c) CA-3.

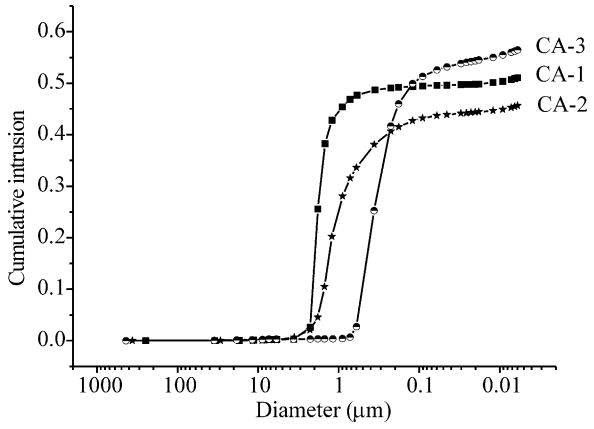


Fig. 2. Cumulative intrusion versus pore diameter plot for the carbon performs.

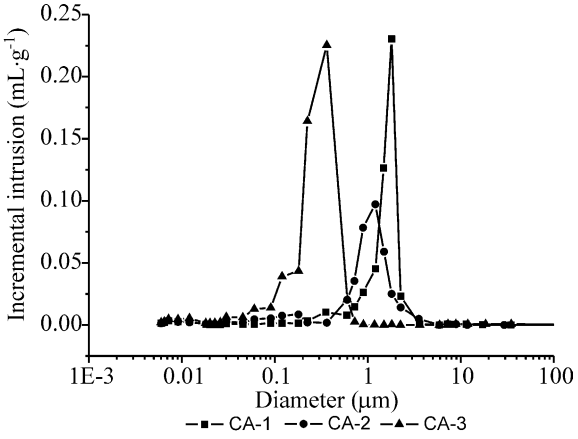


Fig. 3. Incremental intrusion versus pore diameter plot for the carbon performs.

Table 1
The properties of porous carbons preforms

| Sample | Carbon skeletal density ($g \cdot cm^{-3}$) | Porosity (%) | Bulk density ($g \cdot cm^{-3}$) | Average pore size (μm) | BET surface area ($m^2 \cdot g^{-1}$) |
|---|---|---|---|---|---|
| CA-1 | 1.53 | 43.82 | 0.86 | 1.81 | 354 |
| CA-2 | 1.41 | 38.03 | 0.86 | 1.12 | 364 |
| CA-3 | 1.45 | 45.02 | 0.80 | 0.33 | 414 |

and the wetting behavior of the infiltration materials [13,14]. The sample CA-3 has the smallest pore size, but its porosity and BET surface area are larger than those of samples CA-1 and CA-2, which leads to a much higher exothermic reaction temperature. So the preform of CA-3 cracked due to thermal stresses resulting from rapid local heating. These cracks were filled with silicon and were called silicon veins or silicon lakes. In addition, some silicon carbide grains grow during these high temperature excursions, which results in the silicon carbide grain coarsening [Fig. 4(d),(f)].

The X-ray diffraction analysis of RFA-3 is given in Fig. 5. The peaks corresponding to β-SiC and Si are labeled. It is observed that there is a peak at about $2\theta = 27^\circ$ ($d = 3.35$), which is corresponding to (002) diffraction peak of crystalline graphite. This peak is indicated with an arrow marker in Fig. 5. The XRD pattern of the carbon preform CA-3 is shown in Fig. 6. It is

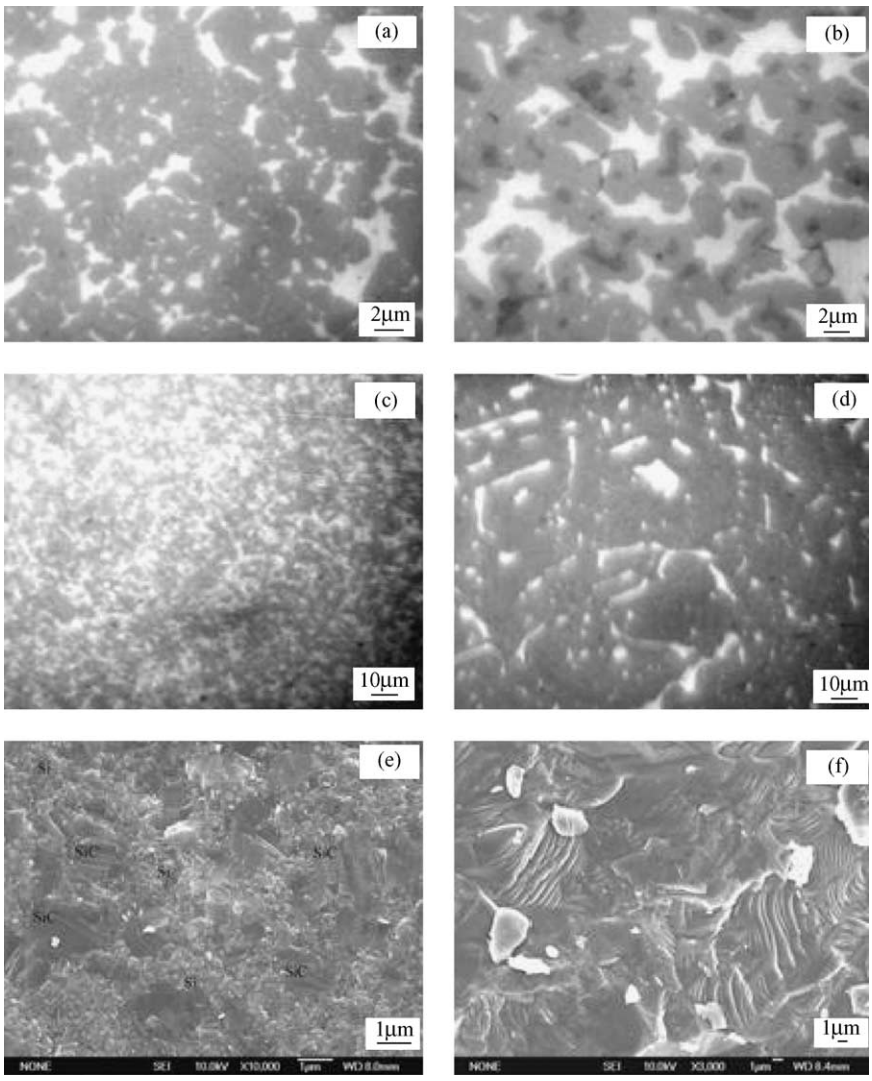


Fig. 4. RFSC optical micrographs (a–d) and SEM micrographs (e–f). (a) Sample RFA-1, (b) sample RFA-2, (c–f) sample RFA-3.

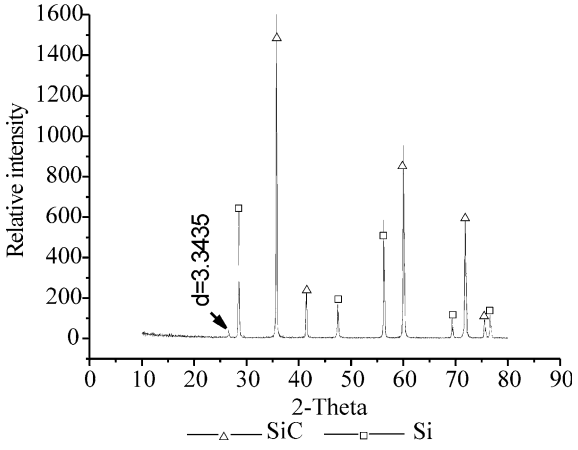


Fig. 5. X-ray diffractogram of sample RFA-3.

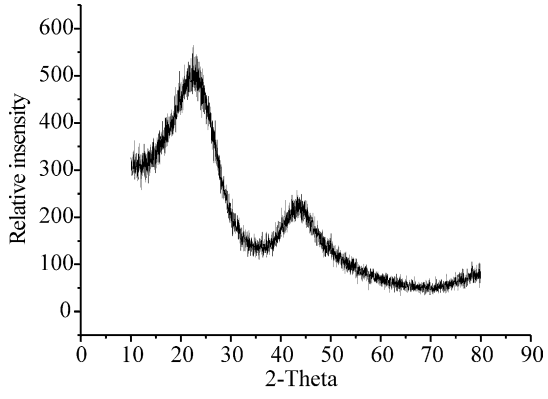


Fig. 6. X-ray diffractogram of porous carbon preform CA-3.

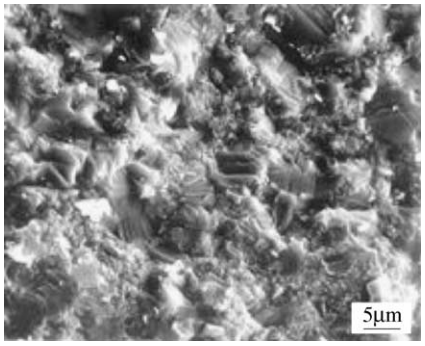


Fig. 7. The fractograph of sample RFA-1.

obvious that the porous carbon possesses mainly an amorphous structure. This suggests that some amorphous carbon became crystalline graphite under the collective influence of high temperature excursions and Si which catalyzes the graphitization reactions.

### 3.3. Mechanical properties of reaction-forming silicon carbide

The room temperature flexural strengths of samples RFA-1, RFA-2 and RFA-3 were 410±30, 240±35 and 145±40 MPa, respectively. Fractographic analysis was conducted by using scanning electron microscopy to characterize the fracture mode and the nature of the flaw origins. In these specimens, flaws included unreacted carbon, residual silicon, pores, and surface damage caused by machining. The sample RFA-1 had a homogenous microstructure and had no residual carbon. However, the sample RFA-2 had some residual carbon and the samples RFA-3 had many silicon veins, so their strengths were lower than that of the sample RFA-1. The failure mode was brittle, and cracks typically originated either at machining flaws at the surface or at unreacted carbon and pore inside the sample. The general feature of a fracture surface in Fig. 7 (the sample RFA-1) shows the typically brittle failure in this material.

## 4. Conclusions

Reaction-formed silicon carbide with controlled microstructure and strength were fabricated by infiltrating pure carbon preforms with molten Si. The effects of carbon preform microstructure on the properties of reaction-formed silicon carbide (RFSC) materials are reported in this paper. The morphology and amount of the residual phases (SiC and C) in the infiltrated material can be tailored according to requirements by careful control of the properties (pore size, porosity and surface area) of the porous carbon preforms. Reaction-formed silicon carbide resulting from infiltrating the preform with an average pore size of about 1.81 μm and a bulk density of 0.86 g $cm^{-3}$ shows the complete conversion of carbon to silicon carbide. The room temperature flexural strength of a reaction-formed silicon carbide with approximately 12 wt.% free silicon is 410±30 MPa. Further improvements in composite properties are possible by controlling the properties of porous carbon preform.

## Acknowledgements

The authors wish to thank Huachang Polymer co., Ltd. for supply of the furfuryl resin, Z.M.Cheng and M.J.Dong for experimental assistance.

## References

[1] T. Hase, H. Suzuki, T. Iseki, Formation process of β-SiC during reaction-sintering, J. Nucl. Mater. 59 (1976) 42–48.
[2] J.N. Ness, T.F. Page, Microstuctural evolution in reaction-bonded silicon carbide, J. Mater. Res. 21 (1986) 1377–1397.
[3] W.B. Hillig, Melt infiltration approach to ceramic matrix composites, J. Am. Ceram. Soc. 71 (2) (1988) C–96-C-99.
[4] H. Zhou, R.N. Singh, Kinetics model for the growth of silicon carbide by the reaction of liquid silicon with carbon, J. Am. Ceram. Soc. 78 (9) (1995) 2452–2456.
[5] T.B. Ramakrishna, Tensile properties and microstructural characterization of Hi-Nicalon SiC/RBSN composites, Ceram. Int. 26 (2000) 535–539.
[6] W.B. Hillig, Making ceramics composites by melt infiltration, Am. Ceram. Soc. Bull. 73 (4) (1994) 56–62.
[7] B.L. Chang, I. Takayoshi, Strength variations of reaction-sintered SiC heterogeneously containing fine-grained β-SiC, J. Mater. Sci. 23 (1998) 3248–3253.
[8] E.E. Hucke, US Patent 3 859 421, 7 January 1975.
[9] L. Hozer, J.R. Lee, Y.M. Chiang, Reaction-infiltrated, net-shape SiC composites, Mater. Sci. Eng., A 195 (1995) 131–143.
[10] M. Singh, D.R. Behrend, Reactive melt infiltration of silicon–molybdenum alloys into microporous carbon performs, Mater. Sci. Eng., A 194 (1995) 193–200.
[11] P. Robert, Y.M. Yang, Liquid-phase reaction-bonding of silicon carbide using alloyed silicon–molybdenum melts, J. Am. Ceram. Soc. 73 (5) (1990) 1193–1200.
[12] R. Pampuch, J. Białoskórski, E. Walasek, Mechanism of ractions in the $Si_l + C_f$ system and the self-propagating high temperature synthesis of silicon carbide, Ceram. Int. 13 (1987) 63–68.
[13] R. Pampuch, E. Walasek, J. Białoskórski, Reaction mechanism in carbon–liquid silicon systems at elevated temperatures, Ceram. Int. 12 (1986) 99–106.
[14] M. Singh, D.R. Behrendt, Reactive melt infiltration of silicon–niobium alloys in microporous carbons, J. Mater. Res. 9 (7) (1994) 1701–1708.